PASJ: Publ. Astron. Soc. Japan **55**, 445–450, 2003 April 25

Galactic Center Shells and a Recurrent Starburst Model

Yoshiaki SOFUE
Institute of Astronomy, The University of Tokyo, Mitaka, Tokyo 181-0015
sofue@ioa.s.u-tokyo.ac.jp

(Received 2002 October 15; accepted 2003 February 5)

Abstract

By applying filtering techniques to remove straight filaments in the 20-cm VLA radio image of the Galactic Center Arc region, we have shown that numerous concentric radio shells of radii 5 to 20 pc are surrounding the Pistol and Sickle region, which we call Galactic Center Shells (GCS). Each shell has thermal energy of the order of 10^{49-50} erg. Several CO-line shells are associated, whose kinetic energies are of the order of 10^{49-50} erg. Summing up the energies of recognized GCSs, the total energy amounts to $\sim 10^{51}$ erg. The GCSs show an excellent correlation with the FIR shells observed at 16–26 μm with the MSX. We propose a model in which GCSs were produced by recurrent and/or intermittent starbursts in the Pistol area during the last million years. The most recent burst occurred some 10^5 years ago, producing an inner round-shaped shell (GCS I); earlier ones a million years ago produced outer shells (GCS II and III), which are more deformed by interactions with the surrounding ISM and Sgr A halo. We argue that recurrent starbursts had also occurred in the past, which produced larger scale hyper-shell structures as well. A burst some million years ago produced the Galactic Center Lobe, and a much stronger one 15 million years ago produced the North Polar Spur.

Key words: Galactic Center — Radio Arc — Radio Shells — Starburst — Star formation

1. Introduction

The Galactic Center radio-continuum Arc comprises a bunch of highly aligned magnetic fields vertical to the galactic plane. Various thermal features, such as the "Sickle" and "Bridge", are superposed (Yusef-Zadeh, Morris 1987a,b). Besides the prominent features, several fainter loops with larger diameters are known to be apparently superposed on the Arc (Yusef-Zadeh, Morris 1987b). However, since the radio emission from the Arc dominates, the faint radio features have not been investigated in details.

In the present work, we tried to enhance the concentric shell structures by applying a filtering technique, which removed straight filaments in the Radio Arc, and showed that the enhanced features comprise numerous thermal radio shells, which we call the Galactic-Center Shells (GCS), in positional coincidence with 16–26 μm infrared shells observed by MSX (Shipman et al. 1997). We also compared the shells with CO-line morphology around the Arc regions using a high-resolution CO survey of the Galactic Center (Oka et al. 1998), while a direct interaction of the CO clouds with the Radio Arc is still controversial.

Based on the obtained images, we propose a new idea that the GCSs are coherent expanding fronts from a starburst in the GC near the Pistol and Quintuplet stars. Starbursts in the Galactic Center (GC) are among the major interesting topics in the history of the activity of the Milky Way. We discuss the GCS as being a manifestation of the most recent starburst in the GC, where past recurrent bursts yielded various scale shells, such as the North Polar Spur (NPS: Sofue 1977, 1994, 2000) and the Galactic-Center Lobe (GCL: Sofue, Handa 1984). We further propose a recurrent starburst model for the GCS, GCL, and NPS.

2. Filtering Technique and Data

We used the VLA 20-cm and 6-cm radio data from Yusef-Zadeh and Morris (1987a,b) with angular resolutions of $16''$ and $2''$, respectively, which are available as an archive in FITS format and are distributed on a CD-ROM (Condon, Wells 1992).

We first applied the radial-relieving method (Sofue 1993), while taking the center at the Sickle (G $0.18-0.04$) position. The radial-relieving method comprises the following procedure. A radio image is slightly enlarged, e.g. by a factor of 1.05, concentric to a position which is supposed to be the center of a shell to be enhanced. The original map is then subtracted from the enlarged map with the center positions coinciding. The difference map gives a relieved residual, enhancing loop-like features concentric to the center position, while other extended features are suppressed. We also used the pressing method (Sofue, Reich 1979) in order to subtract the straight filaments in the Arc, which is the same procedure as that used to remove scanning effects from a radio map, except that the scan-direction is assumed to be parallel to the filaments. We also used a background-filtering technique (Sofue, Reich 1979) in order to subtract the extended background emission, such as that due to the Sgr A halo.

Among the various features abstracted from the data, we have taken those features to be real, only if the amplitudes were significantly greater (e.g. more than 3 times) than the r.m.s. noise of the original image, and the features could be recognized on the original maps as well. Here, the r.m.s. noise was estimated for emissions from the most quiet region in the original map, including the residual interferometer patterns. The radial relieving technique has the potential to enhance artificial concentric patterns. In order to confirm that the enhanced

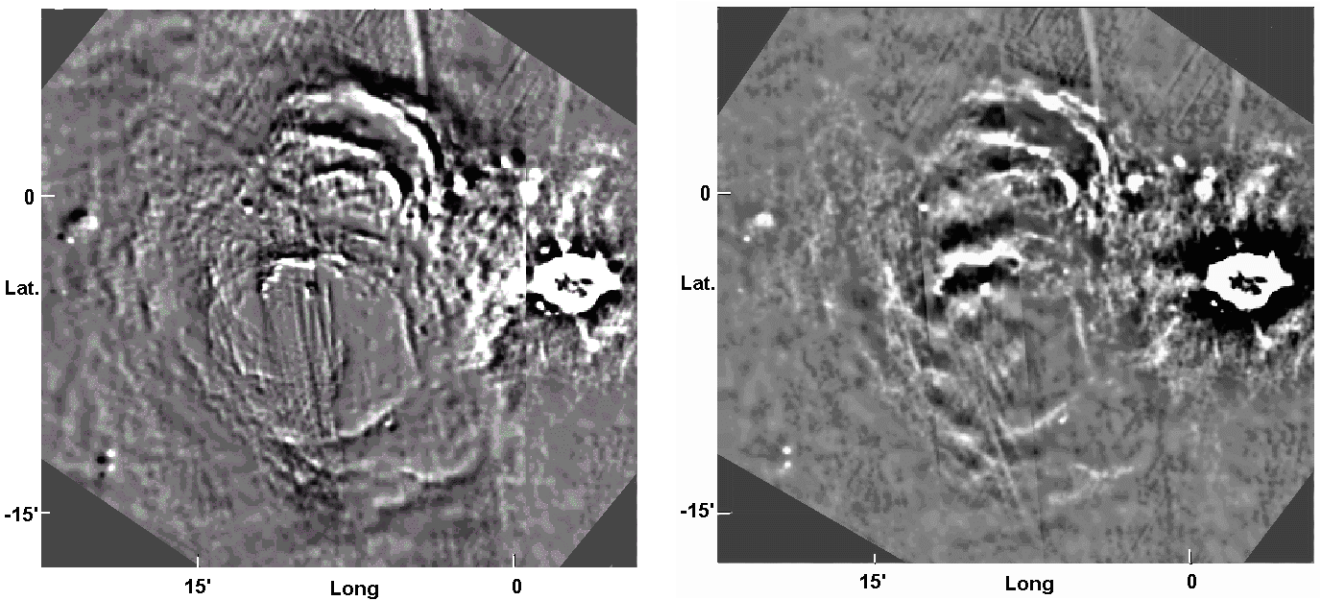

Fig. 1. (a: left) Radial-relieved image of the Galactic Center Arc region observed with the VLA at 20 cm (1.446 GHz: original data from Yusef-Zadeh, Morris 1987a). Numerous loop features are prominent. (b: right) Pressed VLA 20-cm map, where straight Arc filaments have been removed by the pressing method. Extended emissions were also subtracted by a background-filtering technique.

features are real, we cross-checked the result from three different methods: (a) radial relieving to enhance the shell (loop) features, (b) pressing method to remove straight filaments, and (c) background filtering (unsharp masking). The features discussed here are all visible in the three results. They were also confirmed to be visible in the original maps, if their intensities are properly displayed individually.

3. Multiple Radio Shells

3.1. Open Lotus

The results are shown in figures 1 and 2 in galactic coordinates. Figure 1a shows a radial-relieved 20-cm image (original data from Yusef-Zadeh, Morris 1987b); figure 1b is a pressed image, where the vertical filaments have been removed by the pressing method. Figure 2a shows the same as figure 1 in a contour form, and figure 2b is the same but smoothed to an angular resolution of $20''$. In figure 2b we illustrate the positions of the identified loops in superposition on the 20-cm VLA map, and name them as GCS (Galactic Center Shells) I, II and III. We mark the Sickle (Yusef-Zadeh, Morris 1987a,b) by S.

These loops are clearly recognized on the original 20-cm image as well as on the 6-cm images. The fact that the same loop features are recognized in the original 6-cm and 20-cm maps confirms that the loops are not an artifact of the reduction procedure. Note, however, that because their faintest parts are contaminated by various interferometer patterns, we discuss only the global features here.

The most pronounced loop, GCS I, is centered on G 0.170−0.125 at $(l, b) = (0.^\circ170, -0.^\circ125)$ with a radius of $4.'24$, which comprises an almost perfectly round loop. At an assumed distance of the Galactic Center of 8 kpc, this radius corresponds to 9.9 pc. The Sickle (S) at G 0.192−0.62 with a radius of $0.'95$ is apparently in touch with GCS I at the north-western inner edge, and the 'Handle' appears to compose a part of GCS I. The brightest loops, Shells II and III, are coincident with the thermal filaments in the Radio Bridge, which are also concentric to the other loops. In addition to these prominent loop features, there are several segments of loops, or arcs, which are concentric to each other with their centers near to the Sickle and Pistol. They do not necessarily make perfect loops, but are sometimes oval and partial.

Because of their round shapes, these loops are most likely tangential views of multiple shells. The shells appear to compose a coherent structure, suggesting multiple expanding spherical fronts concentric to the Pistol/Sickle region. The galactic-western (negative-longitude) sides of the shells are apparently contacting the halo of Sgr A, and are much brighter than the opposite side. The galactic-eastern sides are less bright, and seem to be expanding more freely with less deformation. As a whole, the shells look like the open petals of a lotus bloom with its neck at the Sgr A halo (figures 2a, b). It is interesting to note that the shells appear to have no clear indication of any interaction with the straight nonthermal filaments in the Radio Arc. In fact, GCS I, the almost perfectly round shell, is not deformed by the Radio Arc.

3.2. Properties of Radio Emission

Most of the GCS are visible in the 43-GHz map (Sofue et al. 1986). The spectral index of the NE part of GCS II, inferred from the 43 GHz and 1.4 GHz intensities, is about ~ -0.05, indicating a thermal origin due to ionized interstellar gas. The typical brightness temperature on GCS II is ~ 50 K at 20 cm, which yields an emission measure of $\sim 1.2\times10^5$ pc cm^{-6}, if the electron temperature is taken to be $\sim 10^4$ K. Assuming that the thickness of the shell is 0.1 times the radius ($0.1\times9.9\,\mathrm{pc}\sim1\,\mathrm{pc}$), the line-of-sight depth will be about ~ 4 pc.

This yields an electron density of $\sim 1.7\times10^2$ cm^{-3}, and a

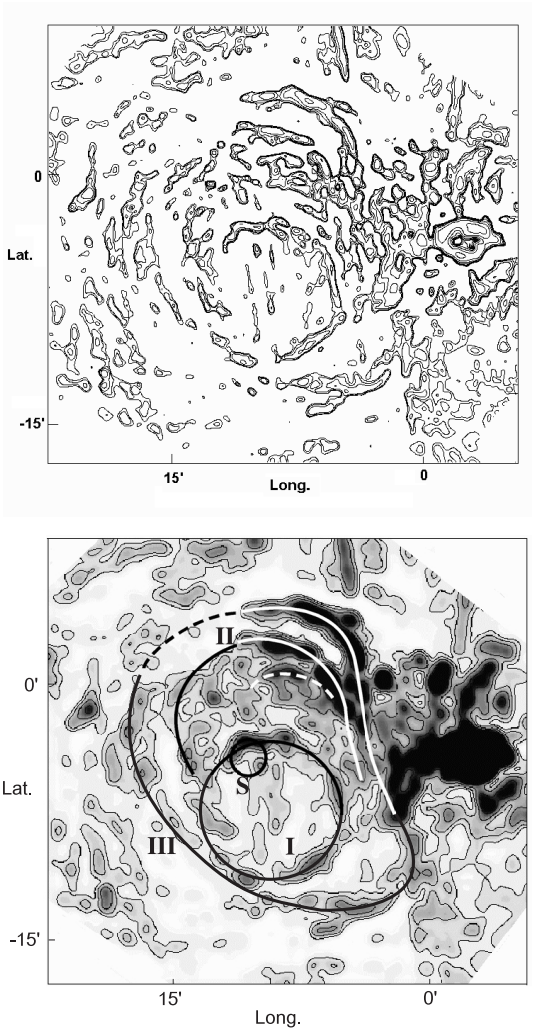

Fig. 2. (a: upper) Same as figure 1a, but in a contour form. Contours are drawn at 1, 2, 4, 8, 16, 32, 64 mJy/(16″ Beam). (b: lower) Same as figure 2a, but in gray scale smoothed to a resolution of 20″. Contours are drawn at 1, 2, 4, 8, 16, 32, 64 mJy/(16″ Beam). GCS I, II, III, and the Sickle (S) are indicated by the full lines.

total mass of the ionized hydrogen $\sim 5 \times 10^3\,M_\odot$. The thermal energy would, then, be $\sim 1 \times 10^{49}$ erg. However, the southern part appears to have a steeper spectrum as inferred from 20 cm and 6 cm maps, although the present data are not sufficiently accurate to derive spectral indices in such faint features. Thus, we cannot exclude the possibility that the shell comprises non-thermal emission, such as a supernova remnant.

3.3. Far-Infrared Shells

GCS I coincides in positions with the most prominent far-infrared loop observed by the MSX experiment at 16–26 μm (Shipman et al. 1997). The MSX image also shows many other shells, coincident with the other GCSs. In figure 3 we compare the radio shells with the MSX image. The association of the FIR emission may indicate that the shells are predominantly thermal, consistent with the radio spectrum, and contain warm dust and probably molecular gas. It is interesting to note that the Arc is not visible in the FIR at all. Thus, the MSX FIR image appears to be very similar to the radio image after subtracting the Arc filaments.

3.4. Molecular Shells

The association of molecular gas with the radio Arc and Bridge has been discussed in details by Serabyn and Guesten (1987). Numerous CO-line shells and arcs are found toward the presently identified GCSs, whereas no clear CO feature is associated with the Arc. Figure 4 shows an unsharp-masked total CO intensity map. Figure 5 shows channel maps of the CO emission. Here, the CO map has been produced using the data cube of the Galactic Center CO survey by Oka et al. (1998). In figure 4, we indicate GCS I, II, III, and the Sickle (S) by full lines.

Tsuboi et al. (1997) have found an expanding shell-like dense molecular cloud of radius $\sim 3'$ centered on $(l, b) = (7', -7')$ at $V_{\rm lsr} = 30\,{\rm km\,s^{-1}}$ in their CS-line observations using the Nobeyama 45-m telescope. The shell's expanding velocity is $20\,{\rm km\,s^{-1}}$, and the kinetic energy of the expansion is estimated to be of the order of 10^{51} erg. They suggest that that the shell may have originated by supernovae $\sim 10^5$ yr ago. The eastern edge of this shell is elongated along the Radio Arc, whereas the western half coincides with the western half of GCS I. This cloud is also visible clearly by CO in figure 5 at $V_{\rm lsr} = 30\,{\rm km\,s^{-1}}$, showing a half-moon shape in GCS I.

Oka et al. (1998, 2001) have noticed an expanding shell at $V_{\rm lsr} = 50\,{\rm km\,s^{-1}}$ with a radius and thickness of ~ 9 pc and ~ 4 pc, respectively, centered on $(l, b) = (15', -4')$. We illustrate this shell by the dotted circle in figures 4 and 5. The CO intensity is roughly $\sim 10^2\,{\rm K\,km\,s^{-1}}$, yielding a molecular mass of $2 \times 10^4\,M_\odot$ for a conversion factor of $1.0 \times 10^{20}\,{\rm H_2\,[K\,km\,s^{-1}]^{-1}}$ (Arimoto et al. 1996). The shell is expanding at $25\,{\rm km\,s^{-1}}$, yielding a kinetic energy of $\sim 1.4 \times 10^{50}$ erg, and an age of $\sim 3.5 \times 10^5$ yr. However, the correlation with the present GCSs is not clear.

Besides this expanding shell, there are several arc-features in the channel maps, some of which appear to be spatially coincident with the GCS positions. GCS I appears to be associated with a CO arc at 10 to $30\,{\rm km\,s^{-1}}$. GCS II is associated with a dense CO arc at 60 to $70\,{\rm km\,s^{-1}}$. The galactic-northern part of GCS III is associated with an extended CO arc at -10 to $-20\,{\rm km\,s^{-1}}$. However, no conclusive physical association can be derived from these coincidences at the present resolution, and we cannot exclude the possibility of a chance coincidence.

3.5. X-Ray Sources in GCS I

The ASCA Galactic Center survey has revealed several bright X-ray sources in the 6.4 keV iron-line (Maeda 1998). The brightest source coincides with Sgr B. The second-strongest source coincides with the Radio Bridge, with which GCS II and III are associated. Most interestingly, the third-strongest source, associated with the Arc region, coincides with the center of GCS I, which is toward the hole in the FIR 16–26 μm emission. An extended continuum X-ray source at 0.7–10 keV is also found near to the center of GCS I.

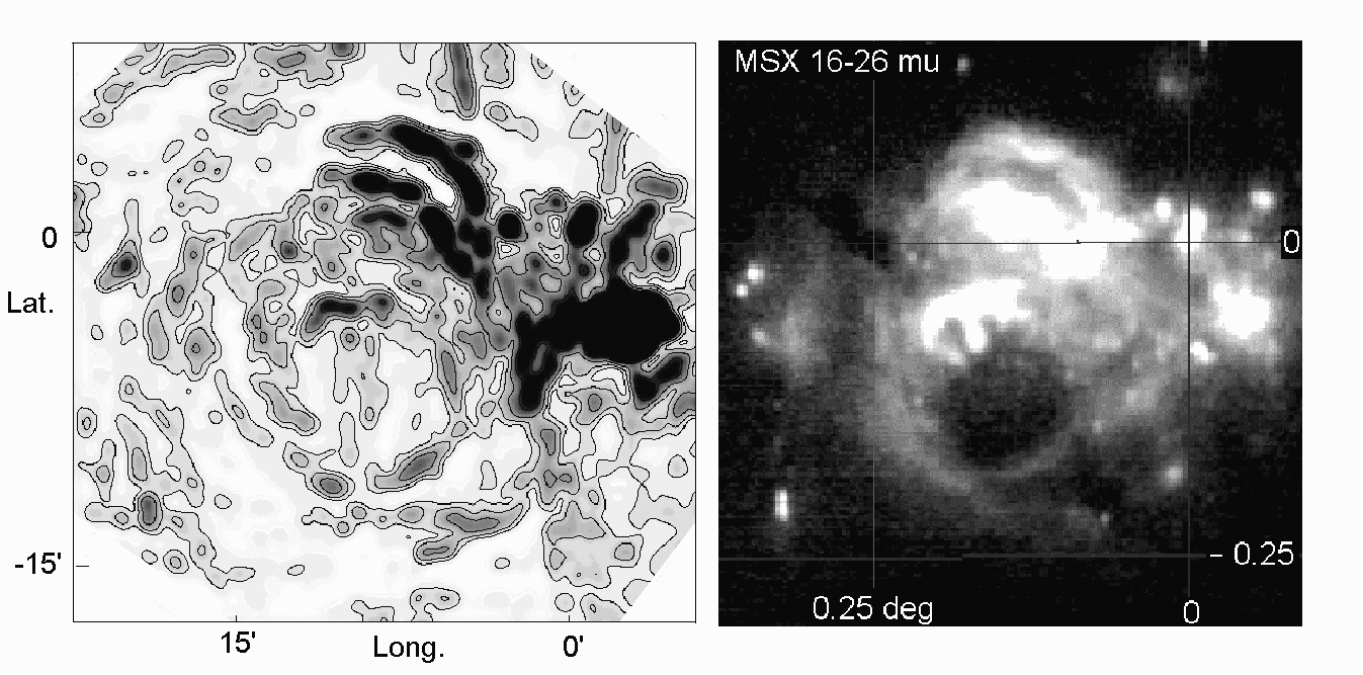

Fig. 3. Comparison of the radio GCSs (left: the same as figure 2b) with the MSX 16–26 μm image (right: reproduced from Shipman et al. 1997).

4. Discussion

4.1. GCS Energetics

The concentric distribution of the GCSs suggests that they have a common origin, most likely due to mass loss or explosions associated with active star formation near to the Pistol and Sickle. In fact, intense star-forming activity has been observed as the Pistol star and Quintuplet stars (Figer et al. 1998, 1999; Lang et al. 1999). Figer et al. (1999) estimate the mass-loss rate and duration to be $10^{-4}\,M_\odot\,\mathrm{yr}^{-1}$ and 6000 yr with a wind velocity of 2000 km s^{-1}, which yields a total kinetic energy of $\sim 2.4\times10^{49}$ erg. This is comparable to the thermal energy of a single GCS and the kinetic energy of an associated CO shell.

If such giant stars, or an ensemble of massive stars, like the Quintuplet, were born recurrently in the past, they would have produced multiple ionization shells, which expanded to sizes as large as several to tens of parsecs. Interactions with and/or the accumulation of background interstellar gas and molecular clouds would decelerate the expansion velocity to several tens of km s^{-1}, as observed in the GCS. Hence, the GCSs would be shells in the evolved phases of similar nebulae to the Pistol. If the total energy E is conserved, the expansion velocity v and radius r are related as $E\sim 2\pi/3\rho r^3v^2$, where ρ is the background gas density. Taking $E\sim 2.4\times10^{49}$ erg, and $v\sim 25$ km s^{-1}, the averaged ISM density is required to be $\rho\sim 20\,\mathrm{H_2\,cm^{-3}}$. The age is of the order of $t\sim r/v\sim 4\times10^5$ yr.

The total energy of the Pistol, Sickle, and all the GCSs identified here is of the order of 10^{51} erg. The age of the outermost shell (GCS III) is estimated to be $\sim 10^6$ yr from their radii of $9'\sim 20$ pc and the assumed expansion velocity of 20 km s^{-1}. We may, thus, suppose that recurrent mini-bursts have occurred

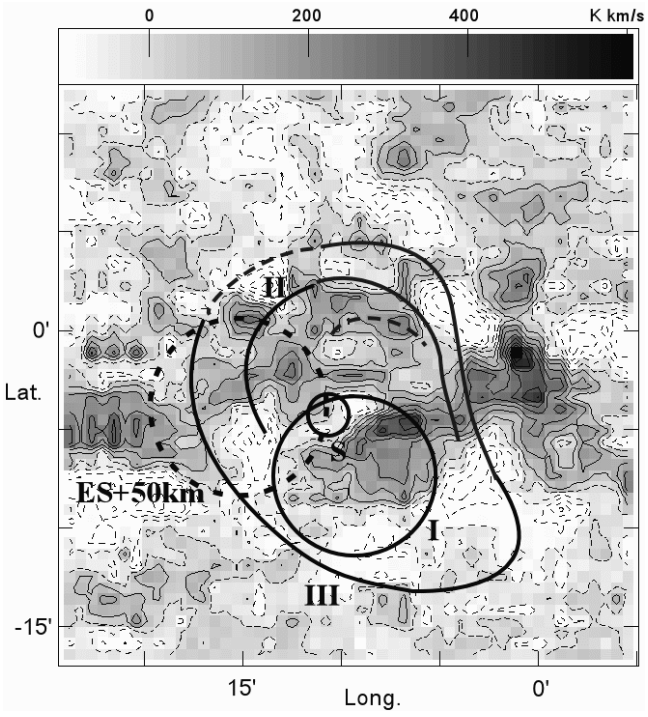

Fig. 4. Unsharp-masked CO integrated-intensity map produced by using the CO survey by Oka et al. (1998). Contour levels are at $6.33\times(1,2,\ldots,10)$ K km s^{-1}. The GCS I, II, III, and the Sickle (S) are indicated by full lines, and the expanding shell of Oka et al. (1998) is indicated by a dotted circle (ES + 50 km).

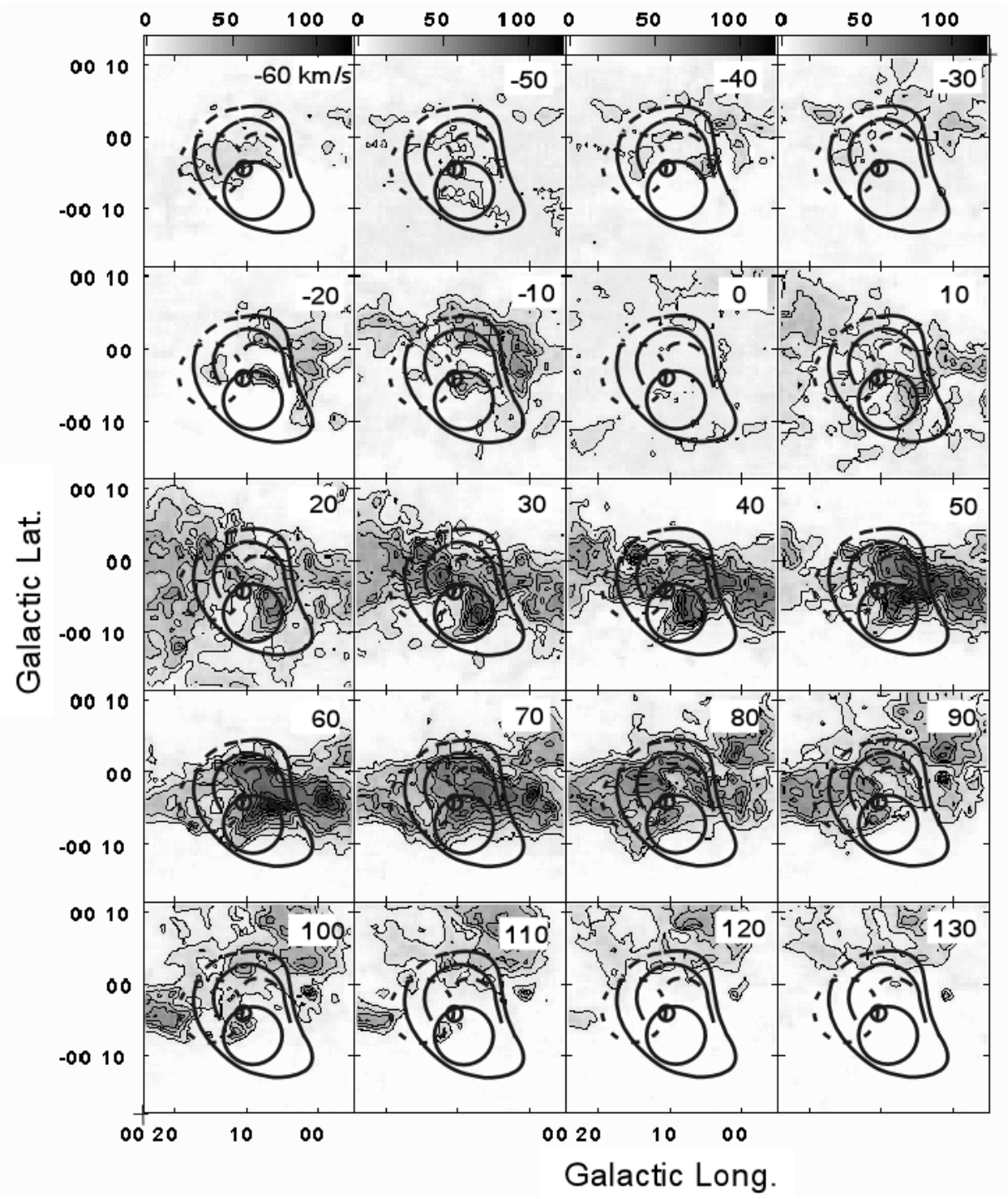

Fig. 5. CO intensity channel maps from Oka et al. (1998) at $V_{\rm lsr} = -60$ to $130\,{\rm km\,s^{-1}}$ at $10\,{\rm km\,s^{-1}}$ interval. The contour levels are at $1.11 \times (1, 2, \ldots, 10)\,{\rm K\,km\,s^{-1}}$. The GCSs are indicated by full lines, and the expanding CO shell by the dotted circle.

near the Pistol/Sickle region in the past million years. The burst centers were within several parsecs of the center of GCS II.

4.2. GCS Morphology

GCS I is almost perfectly round, suggesting that they have not been disturbed very much by the surrounding ISM. However, the outer shells, GCS II and III, are significantly deformed, particularly on their SW side, where they become concave with respect to the shell centers. This fact suggests an interaction with the Sgr A halo. On the contrary, the galactic-eastern sides of GCS II and III are more open, where the shells appear to be torn off into several segments. One prominent segment is indicated by an arc in figure 2b.

If we assume that GCS II, III, and the other segments (as

in figure 2) are a coherent structure, they may be parts of a large shell, which is elongated in the direction perpendicular to the galactic plane, with the galactic-western sides being interrupted by the Sgr A halo and the eastern sides expanding more freely. If the GCSs are expanding shells in the GC gas disk, the vertical elongation is a natural consequence due to the background gas-density distribution. The lopsidedness observed in most of the GCSs will be due to interactions with an inhomogeneous ISM, such as the Sgr A halo and neighboring molecular clouds.

4.3. GCS Origin: Recurrent Starburst Model

We have proposed a bipolar hyper-shell (BHS) model due to an intense energy release, such as starbursts at the GC in order to explain the large-scale radio shell structures associated with the GC (Sofue 1977, 1984, 1994, 2000). This model can be applied to smaller scale shells, such as the GCSs. BHS simulations have shown that an expanding shell is round in the early phase, when the shell radius is smaller than the disk thickness. GCS I may be in such an early phase. Then, the shell becomes elongated in the direction perpendicular to the disk when the radius becomes comparable to the disk thickness. GCS II and III would be in such a phase. Hence, GCSs would manifest sequential phases of evolution of an expanding shell originating around the Pistol.

According to BHS simulations, the shell expands further into the halo, while becoming more elongated and opened to form a bipolar Ω shape or an hour-glass shape. In fact, radio observations have shown an Ω-shaped feature above the Galactic Center, called the Galactic Center Lobe (GCL), which requires energy of the order of 10^{54} erg and an age of $\sim 10^6$ yr (Sofue 1985). If the energy scale is greater, the Ω-shaped shell expands into the halo, forming a larger scale BHS. In fact, in our Galaxy an extremely large shell has indeed been observed in radio and X-rays as the North Polar Spur (NPS), for which the BHS model has been successfully applied; the simulation requires an input energy of $\sim 10^{55}$ erg and an age of $\sim 1.5 \times 10^7$ yr (Sofue 1977, 1984, 1994, 2000). Similar BHS or hyper-wind phenomena have also been observed in starburst galaxies (Heckman et al. 1990), for which a number of numerical simulations have been successfully applied (Tomisaka, Ikeuchi 1988; Suchkov et al. 1994; Strickland, Stevens 2000; Sofue, Vogler 2001).

We, thus, propose a recurrent-starburst model in the Galactic Center. The most recent mini-burst, which occurred $\sim 10^5$ yr ago, produced the inner GCS (I and S). This is in agreement with supernova explosions $\sim 10^5$ yr ago suggested by Tsuboi et al. (1997) and Oka et al. (1998, 2001). The outer GCSs (II and III) were created by previous ones some 10^{5-6} yr ago. Each energy scale of these mini-bursts was of the order of 10^{51} erg. A stronger burst a million years ago produced the Galactic Center Lobe, for which an energy of $\sim 10^{54}$ erg is required. A much bigger burst with $\sim 10^{55}$ erg occurred 15 million years ago, and produced the North Polar Spur. Their energy scales are diverse from 10^{51} to 10^{55} erg. The large, long-living shells, like the GCL and NPS, would not necessarily be due to a single event, but due to the accumulation of succeeding mini-bursts of GCS scale and bursts of GCL scale, respectively.

The radio continuum data were taken from the VLA public images, courtesy Drs. F. Yuzef-Zadeh and M. Morris, distributed by J. J. Condon and D. Wells by a CD-ROM. The author thanks Dr. T. Oka for the CO-line survey data in FITS format.

References

Arimoto, N., Sofue, Y., & Tsujimoto, T. 1996, PASJ, 48, 275
Condon, J. J., & Wells, D. 1992, Images from the Radio Universe (CD-ROM), NRAO
Figer, D. F., Morris, M., Geballe, T. R., Rich, R. M., Serabyn, E., McLean, I. S., Puetter, R. C., & Yahil, A. 1999, ApJ, 525, 759
Figer, D. F., Najarro, F., Morris, M., McLean, I. S., Geballe, T. R., Ghez, A. M., & Langer, N. 1998, ApJ, 506, 384
Heckman, T. M., Armus, L., & Miley, G. K. 1990, ApJS, 74, 833
Lang, C. C., Figer, D. F., Goss, W. M., & Morris, M. 1999, AJ, 118, 2327
Maeda, Y. 1998, PhD Thesis, Kyoto University (ISAS Research Note No. 653)
Oka, T., Hasegawa, T., Sato, F., Tsuboi, M., & Miyazaki, A. 1998, ApJS, 118, 455
Oka, T., Hasegawa, T., Sato, F., Tsuboi, M., & Miyazaki, A. 2001, PASJ, 53, 779
Serabyn, E., & Guesten, R. 1987, A&A, 184, 133
Shipman, R. F., Egan, M. P., & Price, S. D. 1997, Galactic Center News, ed. A. Cotera and H. Falcke, Vol. 5, 3
Sofue, Y. 1977, A&A, 60, 327
Sofue, Y. 1984, PASJ, 36, 539
Sofue, Y. 1985, PASJ, 37, 697
Sofue, Y. 1993, PASP, 105, 308
Sofue, Y. 1994, ApJ, 431, L91
Sofue, Y. 2000, ApJ, 540, 224
Sofue, Y., & Handa, T. 1984, Nature, 310, 568
Sofue, Y., Inoue, M., Handa, T., Tsuboi, M., Hirabayashi, H., Morimoto, M., & Akabane, K. 1986, PASJ, 38, 475
Sofue, Y., & Reich, W. 1979, A&AS, 38, 251
Sofue, Y., & Vogler, A. 2001, A&A, 370, 53
Strickland, D. K., & Stevens, I. R. 2000, MNRAS, 314, 511
Suchkov, A. A., Balsara, D. S., Heckman T. M., & Leitherer, C. 1994, ApJ, 430, 511
Tomisaka, K., & Ikeuchi, S. 1988, ApJ, 330, 695
Tsuboi, M., Ukita, N., & Handa, T. 1997, ApJ, 481, 263
Yusef-Zadeh, F., & Morris, M. 1987a, ApJ, 322, 721
Yusef-Zadeh, F., & Morris, M. 1987b, AJ, 94, 1178